



# Speed of sound index for liver steatosis estimation: a reliability study in normal subjects

Ilias Gatos   
 Petros Drazinos   
 Thanasis Loupas   
 Spyros Yarmenitis   
 John Koskinas   
 Pavlos S. Zoumpoulis 

## PURPOSE

Non-alcoholic fatty liver disease (NAFLD) is the most widespread type of chronic liver disease in the Western countries. Ultrasound (US) is widely used for NAFLD staging. The Resona 7 US system (Mindray Bio-Medical Electronics Co., Ltd.) includes an image optimization and speed of ultrasound-related feature, Sound Speed Index (SSI). SSI is applied in a region of interest (ROI) that could potentially aid in tissue characterization. The purpose of this study is to evaluate the reliability of SSI on various examination parameters on normal subjects.

## METHODS

Twenty normal subjects were examined by two radiologists performing SSI measurements in the liver in different ROI depths and sizes. Intraclass correlation coefficient (ICC) was calculated to measure intra- and inter-observer variability and inter-ROI variability.

## RESULTS

For all ROIs and both radiologists, the mean inter-observer ICC was 0.62 and the mean intra-observer ICC was 0.52 and 0.79. The mean SSI values for all ROIs and examiners were in the range 1528.79-1540.16 m/s.

## CONCLUSION

The results indicate that SSI can lead to reliable measurements on normal subjects, independent of ROI size but dependent on ROI placement. More studies processing NAFLD patients, utilizing reference methods of liver fat quantification either for reliability or correlation with SSI, should be performed to further investigate the relevance of the SSI as a potential biomarker in clinical practice for liver steatosis grading.

Chronic liver disease (CLD) is responsible for approximately 2 million deaths/year worldwide, 1 million of which is due to cirrhosis-related complications and 1 million is due to hepatitis B, C, and hepatocellular carcinoma (HCC).<sup>1</sup> About 2 billion people consume alcohol in regular basis worldwide, and more than 75 million are diagnosed with alcohol-use disorders and are at risk of alcohol-associated liver disease (AALD). Approximately 2 billion adults are obese or overweight and over 400 million have diabetes, which are risk factors for non-alcoholic fatty liver disease (NAFLD) and HCC.<sup>2</sup> Specifically, AALD and NAFLD are the main causes of CLD in Western countries.<sup>3</sup> Significant alcohol consumption or unhealthy dietary patterns may lead to alcoholic or non-alcoholic steatohepatitis (NASH), cirrhosis, and HCC.<sup>4,5</sup> AALD, NAFLD, and NASH are developed due to liver tissue inflammation caused by hepatic steatosis (HS). The term HS includes a wide range of pathological situations that involve triglyceride accumulation into the hepatocyte cytoplasm. HS is commonly observed in clinical practice, and its prevalence is increasing along with the pandemics of obesity and type 2 diabetes mellitus.<sup>6</sup> As the presence of HS may lead to increased probability for development of various clinically important diseases, methods for its accurate assessment in terms of existence and severity are needed.

Liver biopsy (LB), despite being considered as the "Reference Standard" in diagnosing NASH existence and HS severity,<sup>7</sup> has serious limitations. LB is an invasive procedure causing post-operative complications to nearly 30% of patients<sup>8</sup> and is characterized by significant

From the Department of Medical Physics (I.G.), University of Patras, School of Medicine, Rion, Greece; Diagnostic Echotomography SA (I.G., P.D., T.L., S.Y., P.S.Z. ✉ p.zoumpoulis@echomed.gr), Kifissia, Greece; and 2nd Department of Medicine (J.K.), National and Kapodistrian University of Athens, Medical School, Hippokraton Hospital, Greece.

Received 2 February 2021; revision requested 19 March 2021; last revision received 14 July 2021; accepted 28 August 2021.

Publication date: 5 October 2022.

DOI: 10.5152/dir.2022.21019

You may cite this article as: Gatos I, Drazinos P, Loupas T, Yarmenitis S, Koskinas J, Zoumpoulis PS. Speed of sound index for liver steatosis estimation: A reliability study in normal subjects. *Diagn Interv Radiol.* 2022;28(5):418-427.

inter-observer variability.<sup>9</sup> To overcome LB limitations, imaging methods such as computed tomography (CT), magnetic resonance imaging (MRI), and ultrasound (US) have been proposed as alternative or complementary methods for HS assessment.

CT offers fat quantification<sup>10</sup> but exposes patients to radiation and is prone to errors.<sup>10</sup> Proton magnetic resonance spectroscopy and MRI provide high accuracy quantification of liver fat content. The main disadvantages of MRI are the low availability, high cost, and lack of standardization.<sup>11</sup>

US is a widely available imaging modality and the most common method used in the evaluation of HS.<sup>12</sup> It evaluates the presence and estimates the amount of liver fat based mainly on qualitative features, namely liver echogenicity, echo texture, vessel visibility, and beam attenuation. US's low cost and absence of side effects render the method a very useful diagnostic tool for the follow-up of the disease's course.<sup>13</sup> Routine US investigation of HS is performed by qualitative assessment of the B-Mode gray scale image.<sup>14</sup> This estimation is achieved through normal, mild, moderate, and severe HS labeling. A corresponding 0-3 grading

scale where 0 represents normal is used.<sup>15</sup> US B-Mode can depict changes of hepatic appearance when intracellular fat accumulation is above 15%-20%.<sup>13</sup> A positive predictive value of 0.87 has been reported for HS diagnosis by using the increased parenchymal echogenicity as a diagnostic criterion. This value increases to 0.94 if other qualitative criteria are included.<sup>16</sup>

However, several considerable limitations exist. Because of the subjective nature of the visual inspection of the US B-Mode liver image, a significant intra- and inter-observer variability occurs.<sup>17,18</sup> Furthermore, US device dependency results in low repeatability and reproducibility. A range of 62%-77% is reported for the positive predictive value of US liver echogenicity for the detection of steatosis.<sup>13</sup> Moreover, visual inspection is not enough to certainly establish the degree of HS and distinguish this pathology from other, associated with increased parenchymal echogenicity, diffuse liver diseases.<sup>19</sup> US is also susceptible to limited beam penetration in obese patients, a high-risk population for HS development.<sup>13</sup>

Various quantification methods have been developed to produce more objective and accurate HS diagnosis and grading. These include the Sonographic Hepatorenal Index (SHRI), the Controlled Attenuation Parameter (CAP), and US Speed-related Indices. SHRI, which is the ratio of the mean liver brightness over the mean renal cortex brightness, is the most popular quantification method. It tends to be more precise and objective in HS estimation than qualitative methods<sup>20-22</sup> but has limitations regarding the representative areas of measurement.<sup>14,16</sup>

The CAP, which is commercially available by Fibroscan TM (Echosens), is a popular US method, based on US attenuation/depth quantification, that overcomes SHRI's limitations. The attenuation/depth of the US waves propagating through human body is tissue-specific, can be quantified, and may potentially differentiate fatty from normal liver tissue,<sup>23</sup> rendering CAP a reliable and accurate quantification method for HS grading.<sup>24-27</sup>

Another tissue-specific US feature is the speed of the US wave through the medium. Many studies have claimed that US image quality, which depends on the speed of US, can be correlated with tissue differences.<sup>28-30</sup> Research effort has been mainly concentrated on the differentiation between normal liver tissue and fatty liver tissue,

giving promising results.<sup>31-33</sup> Recently, Mindray incorporated a speed for the US method in the Resona 7 US system based on Napolitano et al.'s<sup>31</sup> study. This is an adaptive method that determines the most appropriate US speed by evaluating the image quality of various trial sound speeds and identifying the US speed that provides optimum image quality. Originally, this tool was developed to automatically adjust the image quality, based on the tissue characteristics and the appropriate speed of US, and to offer an optimum image quality to the examiner. However, this technique could potentially be useful as a diagnostic tool for steatosis assessment.

The Resona 7 system offers the possibility to the examiner to select a rectangular region of interest (ROI) on the B-Mode US image and perform a measurement of the speed of US which produces the best image quality for the specified area called Sound Speed Index (SSI). Previously published material<sup>31-33</sup> shows that this method has the potential to provide quantitative insight into tissue properties (especially for the fat content in the liver parenchyma). However, no published material on defining reliability criteria and/or an optimum SSI measurement protocol for its use as a diagnostic tool exists. Before embarking into laborious clinical studies, however, it is essential to document SSI's variability and dependence on various parameters, such as ROI position and size, as well as the number of measurements needed to calculate the mean SSI value. Measuring SSI's reliability in a control group is the first and an important step to evaluate whether it can be reliably used in clinical studies involving patients with NAFLD or NASH and in challenging cases with HS and fibrosis coexistence.

In this study, the SSI parameter's reliability was evaluated, testing various factors that may influence SSI measurements and contributing to the introduction of guidelines for examiners using this technology. In detail, the position and size of the SSI measurement of ROI along with the minimum number of measurements needed for extracting mean values were tested for assessing the reliability of SSI.

## Methods

### Clinical data

Between January 2020 and March 2020, 20 normal subjects were processed. Normal subjects included in this study consisted

### Main points

- Speed of ultrasound can be used to differentiate tissue types by ultrasound B-Mode image quality evaluation and offers a useful alternative to other non-invasive methods, especially for the quantification of hepatic steatosis.
- Speed of Sound Index (SSI), a speed of ultrasound-related tissue quantification technology incorporated in the Resona 7 ultrasound device, that is used for image quality adjustment, may be used for tissue characterization, but its reliability has not yet been validated.
- In this study, the reliability of SSI on 20 healthy subjects was evaluated. SSI measurements taken from regions of interest (ROIs) of variable size and placement were used. Intra- and inter-observer variability among 2 radiologists was calculated.
- The study's findings indicate that SSI can lead to reliable measurements, independent of ROI size on healthy subjects. Changing the position of a small ROI may lead to significantly different measurements on the same acoustic window. Medial large size ROIs and medial small size ROIs have a good inter- and intra-observer agreement, while the proximal small size ROI has a poor inter- and intra-observer agreement.

of healthy volunteers of any age and sex and had the following normal biochemical marker mean values (range): alanine aminotransferase: 17.71 (14-21), aspartate aminotransferase: 19.90 (15-26), gamma-glutamyl transferase: 17.86 (7-34), Serum Alkaline Phosphatase: 72 (38-110), and creatinine: 0.96 (0.70-1.20). Every subject had a body mass index  $<25 \text{ kg/m}^2$  and normal liver findings in the B-Mode ultrasound examination (no visible signs of HS and/or fibrosis). They also had a clear clinical history regarding other types of CLD in order to avoid fibrosis existence that could potentially influence the SSI measurement. Given the invasive nature of LB, the above criteria were deemed adequate to indicate that a subject is healthy.<sup>34</sup> The study group consisted of 11 females and 9 males. The age of the subjects was in a range of 26-77 years with a mean value of 54.65 (standard deviation: 15.02) years and a median of 54 years. No pediatric cases were included in our study group. This study was conducted in accordance with the ethical guidelines of the Helsinki Declaration and was approved by our institutional review board (Review Board, decision/protocol number: 2, date of approval: March, 3, 2020). A written informed consent was obtained from all subjects participating in the study.

#### Examination details

A regular B-Mode US abdomen examination was performed on each patient by 2 expert radiologists (EFSUMB experience level 3) having at least 10 years of experience in US of upper abdomen and 1 year in measuring SSI in the liver. The US examination involving SSI measurement was performed on the Resona 7 US (Mindray Bio-Medical Electronics Co., Ltd.) system using a convex SC5-1U transducer. The SSI examination was performed at the same day for each patient by the 2 examiners who measured the SSI twice, for inter- and intra-observer variability calculation. In detail, the examination process with the radiologists was performed consecutively at the same day and time as follows: each subject was, firstly, examined by examiner 1 and, immediately after, by examiner 2. Each subject was, immediately after, re-examined by examiners 1 and 2, at this order. Each examination lasted about 20 min, and each patient was examined for about 90 min.

The SSI mode provides the opportunity for the examiner to place an ROI of variable size in a tissue area and estimates a

sound speed that is related to the type of this tissue. For each SSI measurement, the patient was asked to be placed in a supine position and raise his/her right arm. The examiner then placed the transducer into an intercostal space and pressed gently to establish a good acoustic window between the patient's ribs. The probe was placed on the longitudinal axis of the intercostal space and good acoustical coupling with the skin was assured. After establishing a good acoustic window, the examiner activated the SSI mode and placed each ROI described below in the corresponding areas for measurement. SSI measurements were performed after the patient was asked to hold his/her breath on the neutral respiratory phase. In detail, all SSI measurements were performed through an intercostal space, usually of the right liver lobe (segment VI). For the purposes of this study, measurements in segment V were also performed to assess whether there is a significant difference between measurements in different liver segments. In this study, 7 groups of measurements were analyzed. The definition of the groups was based on the area of SSI measurement, which fulfilled specific criteria, allowing this study to assess whether ROI size and placement affect SSI measurements (Figure 1).

1. **Entire US image ROI (EUIR):** The SSI measurement is obtained from the entire acoustic window of the US image.
2. **Medial large size ROI (MLSR):** The SSI measurement is obtained by placing a large  $\sim 5 \times 5 \text{ cm}^2$  ROI perpendicularly and  $\sim 1 \text{ cm}$  away from liver capsule.
3. **Medial medium size ROI in segment V (MMSR5):** The SSI measurement is obtained by placing a  $\sim 2.5 \times 5 \text{ cm}^2$  ROI perpendicularly and  $\sim 1 \text{ cm}$  away from liver capsule and, specifically, on the segment V of the liver.
4. **Medial medium size ROI in segment VI (MMSR6):** The SSI measurement is obtained by placing a  $\sim 2.5 \times 5 \text{ cm}^2$  ROI perpendicularly and  $\sim 1 \text{ cm}$  away from liver capsule and, specifically, on the segment VI of the liver.
5. **Proximal small size ROI (PSSR):** The SSI measurement is obtained by placing a small  $\sim 2.5 \times 2.5 \text{ cm}^2$  ROI perpendicularly and  $\sim 1 \text{ cm}$  away from liver capsule.
6. **Medial small size ROI (MSSR):** The SSI measurement is taken by placing a small  $\sim 2.5 \times 2.5 \text{ cm}^2$  ROI perpendicularly and  $\sim 3.5 \text{ cm}$  away from liver capsule.

7. **Distal small size ROI (DSSR):** The SSI measurement is taken by placing a small  $\sim 2.5 \times 2.5 \text{ cm}^2$  ROI perpendicularly and  $\sim 6 \text{ cm}$  away from liver capsule.

The areas described above contained only liver parenchyma, while specifically for the EUIR, the appearance of other organs like the gallbladder and the kidney was avoided as much as possible. All measurements were performed on the segments V and VI of the liver. To avoid factors that could affect SSI measurements, vessels with a larger than  $\sim 0.5 \text{ cm}$  diameter were avoided. A prerequisite for all ROI types was immobility of the liver and the probe in order to avoid potential variability of SSI measurements related to movement.

For each ROI type, 10 SSI measurements were acquired and stored for further analysis. To estimate the minimum number of SSI measurements needed to calculate a valid mean SSI value, mean values were calculated from 3, 5, and 10 SSI values in the order they were taken during the examination. Figure 2 illustrates the combinations of 3, 5, and 10 consecutive SSI measurements. Their mean value was calculated and analyzed to assess whether each mean performs similarly.

The different measurement methods (ROI type and number of measurements) described in the paragraphs above were defined to assess the reliability of the SSI measurement.

#### Statistical analysis

Intraclass correlation coefficient (ICC)<sup>35</sup> and Bland-Altman plots<sup>36</sup> are presented for intra- and inter-observer variability between examiners and for inter-ROI (size and position) variability assessment. Furthermore, mean SSI measurements box plots on each factor are presented to demonstrate the variability of mean SSI measurements. In order to define groups of ROI types that lead to statistically significant differences in mean SSI values, the *P*-values between each pair of different ROIs were calculated. Statistically significant differences between pairs of ROIs entail that these ROIs should not be interchangeably used for SSI measurements or SSI mean value calculation. To further validate the hypothesis that the ROIs can be used interchangeably, we applied 2 methods on the comparison of SSI mean measurement ROI pairs (*P*-values on Table 3) to calculate the overall statistical significance derived from

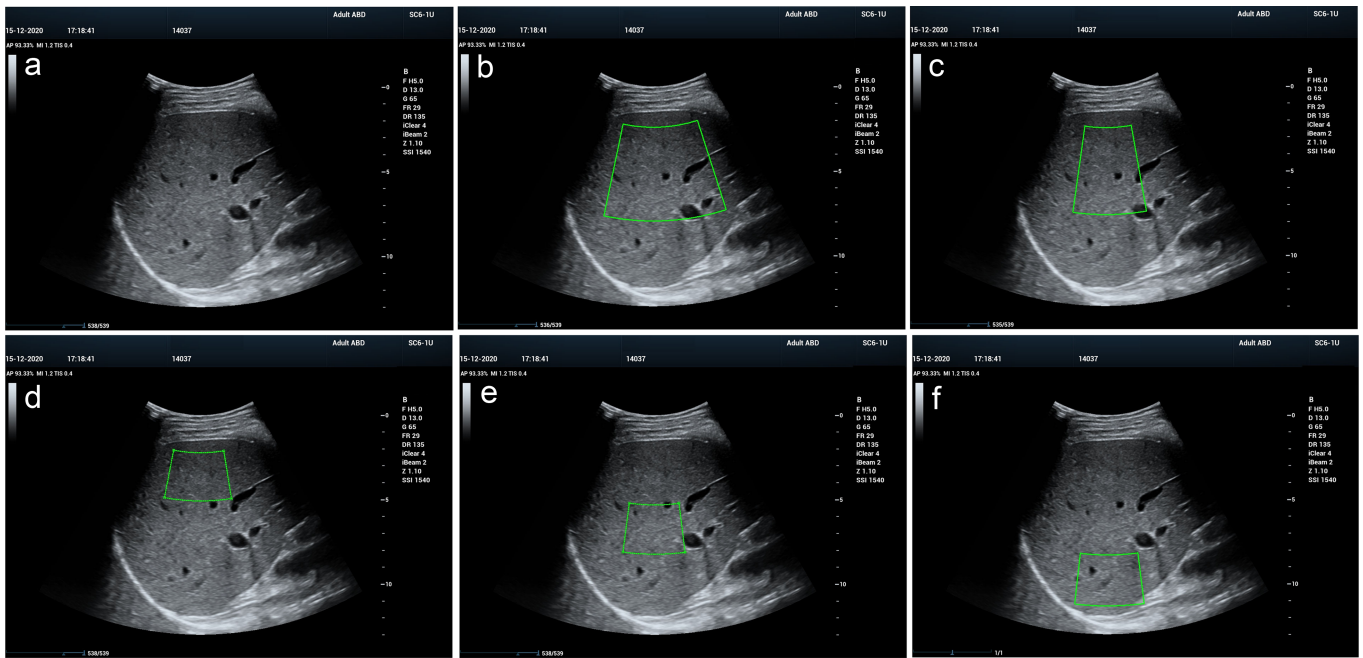


**Figure 1.** Different ROIs chosen from the same acoustic window for SSI measurements. (a) EUR. (b) MLSR. (c) MMSR6. (d) PSSR. (e) MSSR. (f) DSSR. EUR, entire ultrasound image region of interest; MLSR, medial large size region of interest; MMSR5, medial medium size region of interest in segment V; MMSR6, medial medium size region of interest in segment VI; PSSR, proximal small size region of interest; MSSR, medial small size region of interest; DSSR, distal small size region of interest; ROI, region of interest; SSI, Speed of Sound Index.

our one-by-one ROI comparisons. These two methods are the Bonferroni correction<sup>37</sup> and the false discovery rate (FDR).<sup>38</sup> A similar approach was adopted for mean SSI values occurring from 3, 5, and 10 SSI consecutive measurements. In detail, *P*-values of the mean value of each subset of 3 and 5 continuous SSI measurements versus all 10 measurements  $\{X_i, i = 1, 2, \dots, 10\}$  (Figure 2) on all ROIs were calculated and compared. This *P*-value calculation may lead to conclusions regarding whether differences between these mean SSI values are statistically significant and, therefore, whether they can be used interchangeably.

The Python 3.7 programming language was used in this study for all statistical

analysis and figure extraction. In detail, the libraries of Pandas, NumPy, and SciPy were used for all statistical analysis, while Matplotlib and Seaborn libraries were used for graph presentation.

## Results

Intra- and inter-observer variability were measured through ICC values calculation for each ROI. Tables 1-2 show the corresponding results. In Figure 3, Bland-Altman plots of the inter-observer variability of the different ROIs are presented. The statistical significance of the difference between the mean values of SSI measurements obtained from different ROIs was calculated

and is presented in Table 3. Regarding the Bonferroni correction, we defined a type I error rate ( $\alpha$ ) of 0.05. The total number of hypotheses tests is 20. The probability that at least 1 hypothesis will be falsely rejected is  $1 - (1 - \alpha) \times 20$  which equals to 0.64. Hence, the value of  $\alpha$  for each test is set to  $\alpha/20 = 0.0025$ . None of the 20 *P*-values of Table 3 was lower than 0.0025, and therefore, none of the mean value comparison pairs that were tested presented any statistically significant differences using the Bonferroni correction method. Regarding the FDR, none of the 20 tested hypotheses were rejected. Therefore, no statistical significance was detected in any of the mean SSI value comparisons in Table 3. Moreover, the statistical significance of the difference between the mean values of 3, 5, and 10 SSI measurements is presented in Table 4.

The mean absolute difference of the measurements made by the 2 examiners ranged from 0.09 m/s to 2.48 m/s. The ROI with the lowest mean absolute difference was MSSR and the one with the maximum difference was MMSR5. The ICC values that were calculated ranged from 0.3 to 0.86. Concerning intra-observer variability, the range of the absolute mean difference between the 2 measurements for examiner 1 was 0.45-5.23 and 0.13-7.43 for examiner 2.

The box plots of all average SSI measurements per ROI are shown in Figure 4. The

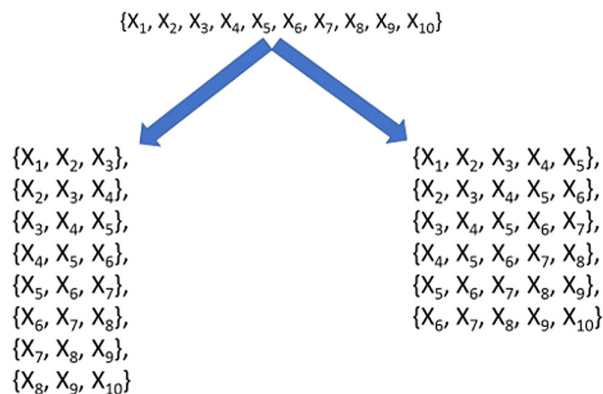


**Figure 2.** Combinations of 3 and 5 consecutive measurements, extracted from 10 SSI measurements performed in the examination process for each subject.

**Table 1.** Results on inter-observer variability on the 20 healthy subjects for each ROI type

Method	Inter-observer variability (examiner 1, examiner 2)						
	EUIR	MLSR	MMSR5	MMSR6	PSSR	MSSR	DSSR
Mean ( $M_1 - M_2$ )	-2.12	1.85	2.11	-2.48	-0.9	-0.09	-2.33
StD	11.45	8.94	4.79	7.19	8.93	6.56	14.63
ICC	0.83	0.66	0.86	0.3	0.58	0.77	0.32
ICC <i>P</i>	.004	.001	<.001	.868	.009	<.001	.107
Slope of least squares	0.86	1	0.94	0.29	0.63	0.78	1

ROI, region of interest; EUIR, entire ultrasound image region of interest; MLSR, medial large size region of interest; MMSR5, medial medium size region of interest in segment V; MMSR6, medial medium size region of interest in segment VI; PSSR, proximal small size region of interest; MSSR, medial small size region of interest; DSSR, distal small size region of interest; M1, measurement from radiologist 1; M2, measurement from radiologist 2; StD, standard deviation; ICC, intraclass correlation coefficient.  
The values were analyzed as the mean value of 10 measurements for each examiner.

mean SSI values for all windows were in the range  $1528.79 \pm 17.52$  to  $1540.16 \pm 10.17$  m/s, where EUIR had the lowest mean SSI value and MMSR5 the highest. The other 6 ROIs, except EUIR, had a tighter range of mean SSI values of  $1533.81 \pm 7.56$  to  $1540.16 \pm 10.17$  m/s. The average SSI measurements per ROI for each examiner are presented in Figure 5. The range of mean SSI measurements for all ROIs were 1527.87-1541.98 m/s for examiner 1 and 1532.44-1539.75 m/s for examiner 2. In detail, mean SSI values with standard deviation and 95% CI of 10 measurements for each ROI type for examiner 1 were EUIR:  $1527.87 \pm 14.55$  (95% CI: 1518.82,1536.92) m/s, MLSR:  $1538.83 \pm 10.98$  (95% CI: 1532.12,1545.54)

m/s, MMSR5:  $1541.80 \pm 10.57$  (95% CI: 1535.23,1548.37) m/s, MMSR6:  $1537.93 \pm 10.40$  (95% CI 1531.09,1544.77) m/s, PSSR:  $1534.25 \pm 9.22$  (95% CI: 1528.62,1539.88) m/s, MSSR:  $1539.70 \pm 10.95$  (95% CI: 1533.01,1546.39) m/s, DSSR:  $1534.54 \pm 7.18$  (95% CI: 1530.00,1539.08) m/s. For examiner 2, the respective measurements were EUIR:  $1532.44 \pm 20.48$  (95% CI: 1506.98,1557.90) m/s, MLSR:  $1536.25 \pm 13.04$  (95% CI: 1526.14,1546.36) m/s, MMSR5:  $1537.62 \pm 10.44$  (95% CI: 1529.52,1545.72) m/s, MMSR6:  $1539.75 \pm 9.77$  (95% CI: 1531.96,1547.54) m/s, PSSR:  $1535.51 \pm 7.55$  (95% CI: 1529.49,1541.53) m/s, MSSR:  $1539.89 \pm 9.81$  (95% CI: 1532.49,1547.29) m/s, DSSR:  $1532.64 \pm 7.94$

**Table 2.** Results on intra-observer variability of examiners 1 and 2 on the 20 healthy subjects for each ROI type

Method	Intra-observer variability (examiner 1—measurements 1, 2)						
	EUIR	MLSR	MMSR5	MMSR6	PSSR	MSSR	DSSR
Mean ( $M_1 - M_2$ )	1.36	-1.29	-0.78	-2.46	-5.23	-0.45	-1.83
StD	24.44	4.94	11.94	12.19	15.54	4.74	9.57
ICC	0.32	0.89	0.62	0.46	0.13	0.91	0.28
ICC <i>P</i>	.761	<.001	<.001	.007	.163	<.001	.068
Slope of least squares	0.39	1.04	0.47	0.41	0.11	0.99	0.42
Method	Intra-observer variability (examiner 2—measurements 1, 2)						
	EUIR	MLSR	MMSR5	MMSR6	PSSR	MSSR	DSSR
Mean ( $M_1 - M_2$ )	-7.43	-0.93	-0.42	-2.31	-0.13	-1.52	-3.57
StD	8.95	4.34	4.95	4.83	9.52	3.03	6.26
ICC	0.85	0.94	0.89	0.86	0.43	0.94	0.65
ICC <i>P</i>	.001	<.001	<.001	<.001	.036	<.001	<.001
Slope of least squares	0.7	1.11	1.13	0.94	0.88	0.86	0.72

ROI, region of interest; EUIR, entire ultrasound image region of interest; MLSR, medial large size region of interest; MMSR5, medial medium size region of interest in segment V; MMSR6, medial medium size ROI in segment VI; PSSR, proximal small size region of interest; MSSR, medial small size region of interest; DSSR, distal small size region of interest; M1, first measurement from radiologist 2; M2, second measurement from radiologist 2; StD, standard deviation; ICC, intraclass correlation coefficient.  
The values were analyzed as the mean value of 10 measurements for each examiner.

(95% CI: 1526.30,1538.98) m/s. The *P*-values of all mean SSI values comparisons in pairs of 2 for each ROI type are presented in Table 3. The intra-observer variability study on the SSI mean values, calculated from groups of 3 and 5 consecutive measurements (Figure 2), compared to the means of 10 measurements, resulted in an ICC = 1 in all ROI types. The corresponding *P*-values are presented in Table 4.

## Discussion

In this study, the reliability of the SSI was assessed for the first time. Twenty normal subjects were processed for liver B-Mode and SSI examination. SSI was measured 10 times for 7 different ROI sizes and positions, for each subject, by 2 examiners. The measurements were analyzed, and measurement variability metrics, such as ICC, were calculated for each ROI.

The inter-observer variability ICC for the different ROIs ranged from 0.3 to 0.86. The intra-observer variability ICC for the different ROIs ranged from 0.13-0.91 to 0.43-0.94 for examiner 1 and examiner 2, respectively. Regarding the inter-observer variability calculation, maximum ICC was obtained from MMSR5 ROI (0.86) and minimum ICC from MMSR6 (0.3) and DSSR (0.32) ROIs. Regarding the intra-observer variability calculation, maximum ICC was obtained from MSSR ROI (0.91 for examiner 1) and both MSSR and MLSR ROIs (0.94 for Examiner 2). On the other hand, minimum ICC was obtained from PSSR (0.13) for the intra-observer variability of the examiner 1. Low intra-observer variability values were calculated for DSSR (0.28) and EUIR (0.32) ROIs for examiner 1. The mean SSI values for all ROIs and examiners were in the range  $1528.79 \pm 17.52$  to  $1540.16 \pm 10.17$  m/s, where EUIR had the lowest mean SSI value and MMSR5 had the highest. The other 6 ROI types had a tighter range of mean SSI values of  $1533.81 \pm 7.56$  to  $1540.16 \pm 10.17$  m/s.

To the best of our knowledge, this is the first study to evaluate reliability metrics for the SSI. Our results show that SSI can be measured with satisfactory reliability on healthy subjects, on variable ROIs and number of measurements. Other newly introduced methods, such as various elastographic techniques, present similar variability on repetitive measurements on different settings.<sup>39-43</sup> A strength of this study is that it evaluates the SSI as a potential biomarker, offering a detailed documentation on its

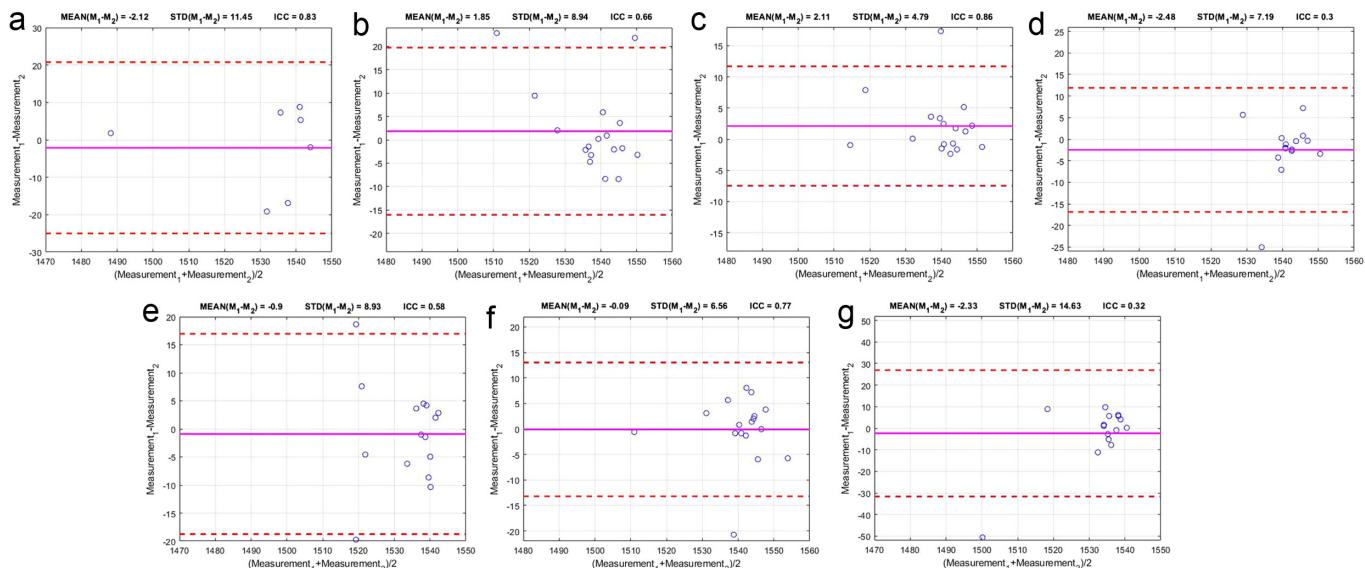


**Figure 3.** Bland–Altman plots for each ROI type. (a) EUIR, (b) MLSR, (c) MMSR5, (d) MMSR6, (e) PSSR, (f) MSSR, and (g) DSSR, presenting inter-observer variability on 20 healthy subjects. The values corresponding to each subject were analyzed as the mean value of 10 measurements for each examiner.

variability due to parameter differentiation, including ROI size and position and number of measurements.

The findings on the variability between SSI measurements by different examiners and in different ROIs may lead to useful insights. Regarding the inter- and intra-observer variability of the 2 examiners among different ROIs, the results indicate that it was more challenging to obtain relatively stable SSI measurements on certain ROIs. The ICC calculated for MMSR6 (0.3) and DSSR (0.32) ROIs was poor for inter-observer variability calculation, while the other ROIs achieved a fair ( $>0.50$  for MLSR and PSSR ROIs) to good ( $>0.75$  for EUIR, MMSR5, and MSSR ROIs) inter-observer variability. Regarding the intra-observer variability, examiner 1 had poor ICC ( $<0.50$ ) for EUIR, MMSR6, PSSR, and DSSR ROIs, while examiner 2 had poor ICC

( $<0.50$ ) only for the PSSR ROI. Both examiners had a near excellent intra-observer variability (ICC  $\sim 0.90$ ) for MLSR and MSSR ROIs. Combining these results, the MSSR ROI seems to produce more stable measurements both for Inter- (ICC = 0.77) and intra-observer variability (ICC = 0.91 and ICC = 0.94 for examiner 1 and examiner 2, respectively). MLSR ROI also produces relatively stable results with inter- (ICC = 0.66) and intra-observer variability (ICC = 0.89 and ICC = 0.94 for examiner 1 and examiner 2, respectively). On the other hand, PSSR ROI seems to have an overall poor inter- (ICC = 0.58) and intra-observer variability (ICC = 0.13 and ICC = 0.43 for examiner 1 and examiner 2, respectively). It is not clear how and why these differences occur between examiners' measurements. Future research should be conducted to further

address SSI measurement limitations. As analyzed in the results section, the SSI variability is not statistically significant for the different ROIs used, except for the EUIR ROI against 3 other ROI variants placed mainly in the center of the acoustic window (MLSR, MMSR6, and MSSR). Significant difference is also observed between MSSR and DSSR ROIs mean SSI values. While these differences are significant between pairs of ROIs using a threshold for statistical significance of 0.05, when the Bonferroni and FDR criteria are used, the ROIs comparison results in non-statistically significant differences in any of the mean SSI value comparisons in Table 3. Although this is an indication that all ROIs may be used interchangeably, more experiments with a larger sample would confirm these findings. Furthermore, only a direct comparison of SSI to steatosis grading assessed by LB histologic examination would evaluate the most accurate SSI ROI variable for liver steatosis estimation.

It should be noted that the EUIR ROI mean value (1528.79 m/s) is lower than the expected theoretical value, while the mean values of other ROIs which range from 1533.81 to 1540.16 m/s are closer to the theoretical values for normal human livers ( $\sim 1560$ – $1580$  m/s).<sup>30,33,44–46</sup> This can be an indication that the latter ROIs' measurements may be more reliable as they are closer to the theoretically measured sound speed for normal liver tissue.<sup>30,33,44–46</sup> These methods, however, had significantly different materials and methodology (e.g., extracted livers from deceased

**Table 3.** *P*-values of all mean SSI values comparisons in pairs of 2 for each ROI type

	EUIR	MLSR	MMSR5	MMSR6	PSSR	MSSR	DSSR
EUIR	-	<b>0.047</b>	0.092	<b>0.047</b>	0.107	<b>0.040</b>	0.182
MLSR	<b>0.047</b>	-	0.284	0.641	0.424	0.780	0.051
MMSR5	0.092	0.284	-	0.338	0.685	0.295	0.198
MMSR6	<b>0.047</b>	0.641	0.338	-	0.503	0.714	0.144
PSSR	0.107	0.424	0.685	0.503	-	0.443	0.268
MSSR	<b>0.040</b>	0.780	0.295	0.715	0.443	-	<b>0.033</b>
DSSR	0.182	0.051	0.198	0.144	0.268	<b>0.033</b>	-

ROI, region of interest; SSI, Speed of Sound Index; EUIR, entire ultrasound image region of interest; MLSR, medial large size region of interest; MMSR5, medial medium size region of interest in segment V; MMSR6, medial medium size region of interest in segment VI; PSSR, proximal small size region of interest; MSSR, medial small size region of interest; DSSR, distal small size region of interest.

Statistically significant differences (*P*-value  $< .05$ ) are shown in bold.

**Table 4.** P-values assessing intra-observer variability on the 20 healthy subjects for the mean value of each subset of 3 and 5 continuous SSI measurements vs. the whole of 10 measurements { $X_i, i = 1, 2, \dots, 10$ } on all ROIs

ROI types	P	
	5 vs. 10 measurements	3 vs. 10 measurements
<b>EUIR</b>	.910	1
	.927	.709
	.775	.975
	.626	.750
	.748	.606
	.695	.590
		.687
	.883	
<b>MLSR</b>	.914	1
	.849	.620
	.770	.789
	.775	.708
	.828	.784
	.975	.832
		.863
	.867	
<b>MMSR5</b>	.654	1
	.650	.319
	.651	.500
	.650	.505
	.321	.500
	.318	.333
		.334
	.316	
<b>MMSR6</b>	.508	1
	.535	.530
	.829	.487
	.810	.481
	.783	.434
	.775	.694
		.687
	.267	
<b>PSSR</b>	.662	1
	.664	.413
	.663	.413
	.664	.523
	.662	.527
	.343	.527
		.446
	.453	
<b>MSSR</b>	.780	1
	.835	.734
	.882	.864
	.970	.803
	.908	.638
	.741	.848
		.629
	.979	
<b>DSSR</b>	.570	1
	.585	.420
	.640	.405
	.306	.527
	.230	.318
	.189	.217
		.175
	.233	

ROI, region of interest; EUIR, entire ultrasound image region of interest; MLSR, medial large size region of interest; MMSR5, medial medium size region of interest in segment V; MMSR6, medial medium size region of interest in segment VI; PSSR, proximal small size region of interest; MSSR, medial small size region of interest; DSSR, distal small size region of interest.

Three and 5 continuous measurements of 10 are ({ $X_1, X_2, X_3$ }, { $X_2, X_3, X_4$ }, { $X_3, X_4, X_5$ }, { $X_4, X_5, X_6$ }, { $X_5, X_6, X_7$ }, { $X_6, X_7, X_8$ }, { $X_7, X_8, X_9$ } and { $X_8, X_9, X_{10}$ }), and ({ $X_1, X_2, X_3, X_4, X_5$ }, { $X_2, X_3, X_4, X_5, X_6$ }, { $X_3, X_4, X_5, X_6, X_7$ }, { $X_4, X_5, X_6, X_7, X_8$ }, { $X_5, X_6, X_7, X_8, X_9$ }, and { $X_6, X_7, X_8, X_9, X_{10}$ }), respectively.

subjects, use of phantoms, etc.), and therefore, comparisons should be made with caution. Moreover, a constant value of 1540 m/s is, usually, used as default in US systems for US beam delay calculation. Defocusing, however, can lead to bad image quality due to the mismatch between the default value of 1540 m/s and actual tissue sound speed. Therefore, a possible mismatch between the measured speeds in this study and the normal liver theoretical speeds could also be due to this reason. Our results did not show statistically significant difference in mean SSI for 3 and 5 vs. 10 measurements. This suggests that a reliable mean SSI calculation can be obtained with fewer than 10 measurements in healthy livers, reducing the examination duration.

Combining the above information, the following recommendations are provided for an appropriate ROI choice and, therefore, for reliable SSI measurements. The MSSR ROI seems to be the most suitable ROI for reliable SSI measurements. The MLSR ROI could be, alternatively, used. On the other hand, the PSSR ROI shows a poor inter- (ICC = 0.58) and intra-observer variability (ICC < 0.5) and should be, therefore, avoided. The mean of 3 SSI measurements is enough to provide a result equivalent to the mean of 5 or 10 measurements.

A limitation of this study is that it was held on healthy subjects only. Our results may, therefore, not apply to patients with higher degree of liver steatosis, where measurement variability may be higher. This variability may affect the ability of SSI to be used as a diagnostic tool for NAFLD assessment as the extent of SSI measurement overlap between healthy subjects and patients with NAFLD or NASH is not evaluated in this article. SSI's diagnostic performance is a task for a future study that may use our findings on SSI measurements. Patients with NAFLD or NASH were not enrolled because a non-homogeneous distribution of liver steatosis or presence of fibrosis could be a confounding factor in assessing the reliability of SSI measurements. First-step parameter evaluation studies rely on normal/healthy "ground truth" groups without making assumptions that studies using LBs as "Gold Standard" do.<sup>20-22,25,27,43,47-48</sup>

Another limitation is that although both examiners tried their best to avoid instability of the acoustic window, a small difference between acoustic window and ROI position used for measurements could still

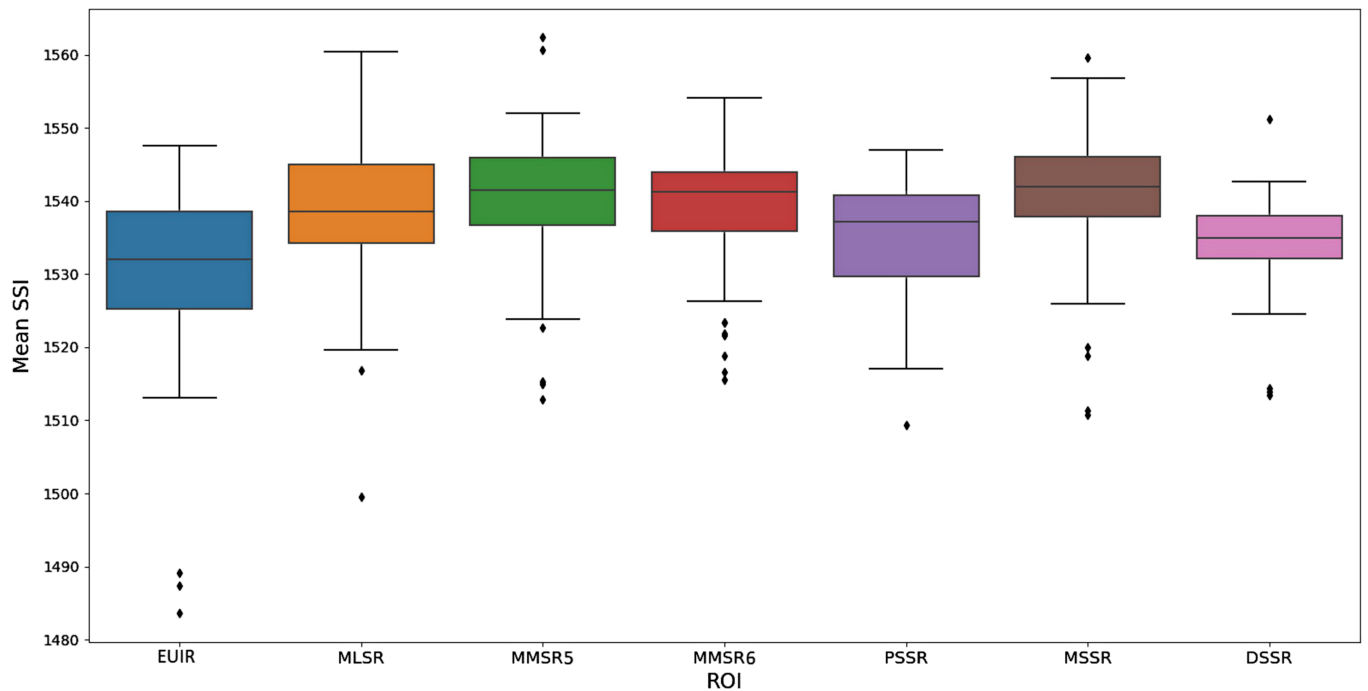


Figure 4. Box plots of SSI measurements along different ROI sizes and positions.

exist. As a result, the acoustic window and various ROIs used for the sets of measurements could vary slightly along the sets of 10 measurements for each patient. This may have added extra variability in the metrics used for measuring SSI reliability. Moreover, the impact of the tissue between the transducer and the SSI measurement ROI was

not directly assessed. Observations by Jakovljevic et al.<sup>44</sup> showed that different tissue type between the transducer and measurement ROI may significantly influence measurements of different depths on phantoms. The fact that the PSSR measurements did not have significantly different average compared to MSSR and DSSR averages

(different depth but same size ROIs from the same acoustic window), but MSSR and DSSR had significantly different averages between them, may confirm Jakovljevic et al.'s findings,<sup>44</sup> who indicated that tissue between the transducer and the ROI influences SSI's measurements and their reliability on human livers. This limitation may

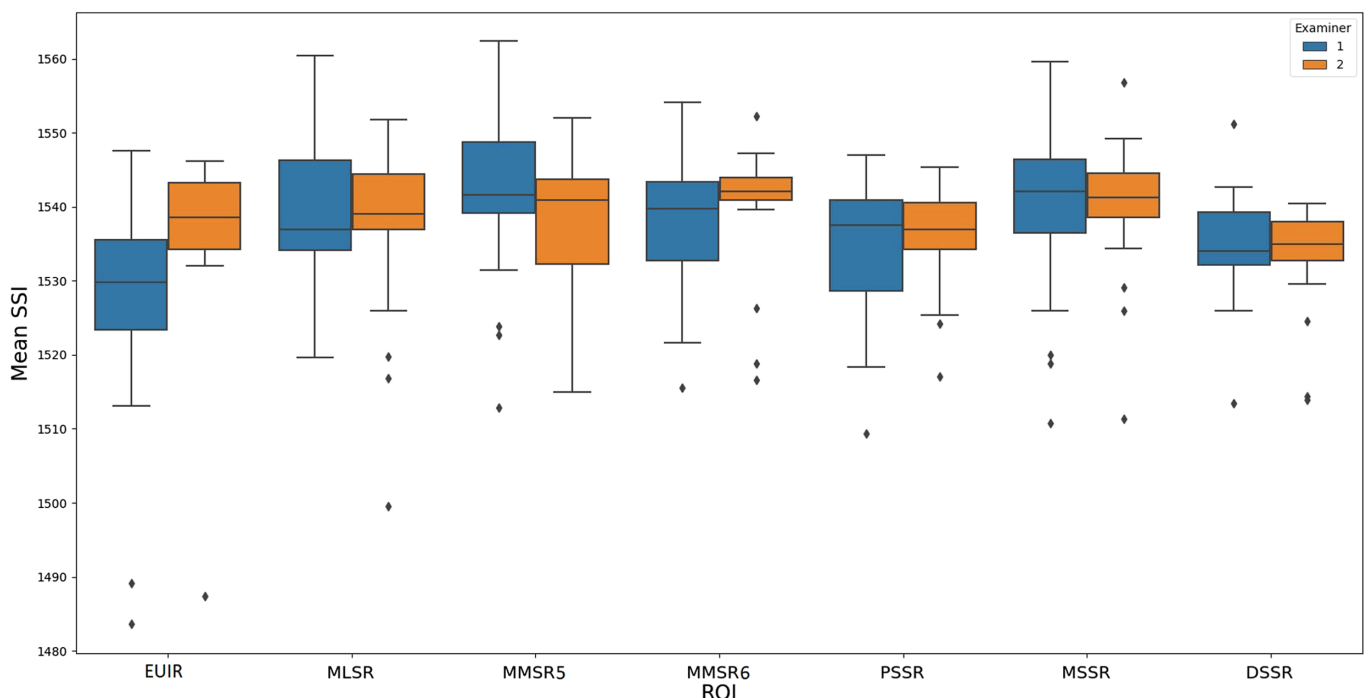


Figure 5. Box plots of SSI measurements along different ROI sizes and positions for each examiner. Examiner 1 and 2 measurement box plots are represented in blue and orange colors, respectively.

be amplified if patients of variable NAFLD or NASH severity are processed, instead of healthy subjects. NAFLD and NASH patients are often characterized by increased subcutaneous fat, which would mean an increase of interlayering tissue between the probe and the liver.<sup>49</sup> It is unclear, however, why PSSR measurements' average is not significantly different than the MSSR and DSSR ROIs given that the distance between PSSR and DSSR is higher than the MSSR and DSSR. Further research on this field may enlighten the impact of the intervening tissue between the transducer and the ROI on human subjects.

The range of mean SSI values acquired from the investigated ROIs was relatively close to the theoretical expected values for healthy liver tissue of (~1560-1580 m/s), indicating the validity of the method. Patients with NAFLD and subcutaneous fat may pose difficulties to the examination protocol, especially on studies evaluating a measurement's reliability. Obesity often prevents the examiner from obtaining a clear acoustic window, rendering the US liver examination, and performing SSI measurements, challenging.

Another limitation is that our sample probably does not represent the full spectrum of the population characterized as normal regarding liver fat quantity. The sample size (20 healthy subjects and 2 independent raters), although small, is above the minimum requirements for reliability studies.<sup>50</sup> Assessment of SSI reliability could, however, be improved in a future study with a larger sample size of test subjects and US operators.

As subcutaneous fat existence and other NAFLD-related factors may strongly influence SSI measurements and their variance, a future study may further evaluate the SSI index and define its limits in NAFLD patients. A comparison of SSI's correlation with LB or MRI-PDF may validate SSI's clinical performance in assessing quantity of liver fat and, therefore, render it an alternative, non-invasive method for NAFLD-NASH grading. The impact of fibrosis coexistence with steatosis could also be investigated as it is challenging for radiologists to define it by visual inspection.<sup>13</sup>

Concluding, SSI is a commercially available non-invasive tool developed for improving US B-Mode image quality that can also be potentially used for liver fat quantification. In this study, the reliability of SSI on healthy subjects was evaluated. The study showed that this tool can lead

to reliable measurements, independent of ROI size on healthy subjects. The mean value of 3 SSI measurements is enough to provide a result equivalent to the mean of 5 or 10 measurements. A good inter- and intra-observer agreement was calculated on MLSR and MSSR ROIs. A poor inter- and intra-observer agreement was calculated on PSSR ROI. Changing the position of a small ROI may lead to significantly different measurements on the same acoustic window. Indeed, the MSSR and DSSR ROIs SSI measurements had statistically significant differences, possibly due to impact of the tissue between the transducer and the ROI. When the Bonferroni and FDR criteria are used, all ROIs present non-statistically significant differences. All ROIs' SSI mean values tested, except the EUIR, were near the theoretical optimum speed of sound values for normal liver tissue. More studies processing NAFLD patients either for reliability or correlation with reference methods of liver fat quantification should be performed to further investigate the relevance of the SSI as a potential biomarker in clinical practice for liver steatosis grading.

#### Acknowledgments

The authors would like to acknowledge the help of Mindray which provided a Resona 7 (Mindray Bio-Medical Electronics Co., Ltd., Shenzhen, China) US system as a loan which made this study possible. Also, the authors would like to acknowledge the contribution to this work from Spyros P. Zoumpoulis who helped in English proofing and editing.

#### Conflict of interest disclosure

Diagnostic Echotomography SA has undertaken a research project (limited to the sharing of clinical feedback) on behalf of the US equipment manufacturer company, Mindray.

#### References

1. Mokdad AA, Lopez AD, Shahraz S, et al. Liver cirrhosis mortality in 187 countries between 1980 and 2010: a systematic analysis. *BMC Med.* 2014;12:145. [CrossRef]
2. Asrani SK, Devarbhavi H, Eaton J, Kamath PS. Burden of liver diseases in the world. *J Hepatol.* 2019;70(1):151-171. [CrossRef]
3. Younossi ZM, Stepanova M, Afendy M, et al. Changes in the Prevalence of the Most Common Causes of Chronic Liver Diseases in the United States from: 1988 to 2008. *Clin. Gastroenterol. Hepatol. Off. Clin. Pract. J. Am. Gastroenterol. Assoc.* 2011;9(6):524-530.e1.

4. Farrell GC, Larter CZ. Nonalcoholic fatty liver disease: from steatosis to cirrhosis. *Hepatology.* 2006;43(2):S99-S112. [CrossRef]
5. Starley BQ, Calcagno CJ, Harrison SA. Nonalcoholic fatty liver disease and hepatocellular carcinoma: a weighty connection. *Hepatology.* 2010;51(5):1820-1832. [CrossRef]
6. Chitturi S, Farrell GC, George J. Non-alcoholic steatohepatitis in the Asia-Pacific region: future shock? *J Gastroenterol Hepatol.* 2004;19(4):368-374. [CrossRef]
7. Joy D, Thava VR, Scott BB. Diagnosis of fatty liver disease: is biopsy necessary? *Eur J Gastroenterol Hepatol.* 2003;15(5):539-543. [CrossRef]
8. Rockey DC, Caldwell SH, Goodman ZD, Nelson RC, Smith AD, American Association for the Study of Liver Diseases. Liver biopsy. *Hepatology.* 2009;49(3):1017-1044. [CrossRef]
9. Ratziu V, Charlotte F, Heurtier A, et al. Sampling variability of liver biopsy in nonalcoholic fatty liver disease. *Gastroenterology.* 2005;128(7):1898-1906. [CrossRef]
10. Limanond P, Raman SS, Lassman C, et al. Macrovesicular hepatic steatosis in living related liver donors: correlation between CT and histologic findings. *Radiology.* 2004;230(1):276-280. [CrossRef]
11. Guiu B, Loffroy R, Hillon P, Petit JM. Magnetic resonance imaging and spectroscopy for quantification of hepatic steatosis: urgent need for standardization! *J Hepatol.* 2009;51(6):1082-1083. [CrossRef]
12. Mishra P, Younossi ZM. Abdominal ultrasound for diagnosis of nonalcoholic fatty liver disease (NAFLD). *Am J Gastroenterol.* 2007;102(12):2716-2717. [CrossRef]
13. Lupşor-Platon M, Stefănescu H, Mureşan D, et al. Noninvasive assessment of liver steatosis using ultrasound methods. *Med Ultrason.* 2014;16(3):236-245. [CrossRef]
14. Chen CL, Cheng YF, Yu CY, et al. Living donor liver transplantation: the Asian perspective. *Transplantation.* 2014;97(suppl 8):S3. [CrossRef]
15. Gerstenmaier JF, Gibson RN. Ultrasound in chronic liver disease. *Insights Imaging.* 2014;5(4):441-455. [CrossRef]
16. Mathiesen UL, Franzén LE, Åselius H, et al. Increased liver echogenicity at ultrasound examination reflects degree of steatosis but not of fibrosis in asymptomatic patients with mild/moderate abnormalities of liver transaminases. *Dig Liver Dis Off J Ital Soc Gastroenterol Ital Assoc Study Liver.* 2002;34(7):516-522. [CrossRef]
17. Hernaez R, Lazo M, Bonekamp S, et al. Diagnostic accuracy and reliability of ultrasonography for the detection of fatty liver: a meta-analysis. *Hepatology.* 2011;54(3):1082-1090. [CrossRef]
18. Strauss S, Gavish E, Gottlieb P, Katsnelson L. Interobserver and intraobserver variability in the sonographic assessment of fatty liver. *AJR Am J Roentgenol.* 2007;189(6):W320-W323. [CrossRef]
19. Taylor KJ, Gorelick FS, Rosenfield AT, Riely CA. Ultrasonography of alcoholic liver disease with histological correlation. *Radiology.* 1981;141(1):157-161. [CrossRef]
20. Borges VFde AE, Diniz ALD, Cotrim HP, Rocha HLOG, Andrade NB. Sonographic hepatorenal ratio: a noninvasive method to diagnose nonalcoholic steatosis. *J Clin Ultrasound.* 2013;41(1):18-25. [CrossRef]

21. Marshall RH, Eissa M, Bluth EI, Gulotta PM, Davis NK. Hepatorenal index as an accurate, simple, and effective tool in screening for steatosis. *AJR Am J Roentgenol.* 2012;199(5):997-1002. [\[CrossRef\]](#)
22. Webb M, Yeshua H, Zelber-Sagi S, et al. Diagnostic value of a computerized hepatorenal index for sonographic quantification of liver steatosis. *AJR Am J Roentgenol.* 2009;192(4):909-914. [\[CrossRef\]](#)
23. Chivers RC, Hill CR. Ultrasonic attenuation in human tissue. *Ultrasound Med Biol.* 1975;2(1):25-29. [\[CrossRef\]](#)
24. Sasso M, Beaugrand M, de Ledinghen V, et al. Controlled attenuation parameter (CAP): a novel VCTE™ guided ultrasonic attenuation measurement for the evaluation of hepatic steatosis: preliminary study and validation in a cohort of patients with chronic liver disease from various causes. *Ultrasound Med Biol.* 2010;36(11):1825-1835. [\[CrossRef\]](#)
25. Myers RP, Pollett A, Kirsch R, et al. Controlled attenuation parameter (CAP): a noninvasive method for the detection of hepatic steatosis based on transient elastography. *Liver Int.* 2012;32(6):902-910. [\[CrossRef\]](#)
26. de Ledinghen V, Vergniol J, Foucher J, Merrerouche W, le Bail B. Non-invasive diagnosis of liver steatosis using controlled attenuation parameter (CAP) and transient elastography. *Liver Int.* 2012;32(6):911-918. [\[CrossRef\]](#)
27. Shi KQ, Tang JZ, Zhu XL, et al. Controlled attenuation parameter for the detection of steatosis severity in chronic liver disease: a meta-analysis of diagnostic accuracy. *J Gastroenterol Hepatol.* 2014;29(6):1149-1158. [\[CrossRef\]](#)
28. Shin HC, Prager R, Gomersall H, Kingsbury N, Treece G, Gee A. Estimation of speed of sound in dual-layered media using medical ultrasound image deconvolution. *Ultrasonics.* 2010;50(7):716-725. [\[CrossRef\]](#)
29. Boozari B, Potthoff A, Mederacke I, et al. Evaluation of sound speed for detection of liver fibrosis: prospective comparison with transient dynamic elastography and histology. *J Ultrasound Med.* 2010;29(11):1581-1588. [\[CrossRef\]](#)
30. Bamber JC, Hill CR, King JA. Acoustic properties of normal and cancerous human liver—II Dependence on tissue structure. *Ultrasound Med Biol.* 1981;7(2):135-144. [\[CrossRef\]](#)
31. Napolitano D, Chou CH, McLaughlin G, et al. Sound speed correction in ultrasound imaging. *Ultrasonics.* 2006;44(suppl 1):e43-e46. [\[CrossRef\]](#)
32. Cho MH, Kang LH, Kim JS, Lee SY. An efficient sound speed estimation method to enhance image resolution in ultrasound imaging. *Ultrasonics.* 2009;49(8):774-778. [\[CrossRef\]](#)
33. Imbault M, Faccinnetto A, Osmanski BF, et al. Robust sound speed estimation for ultrasound-based hepatic steatosis assessment. *Phys Med Biol.* 2017;62(9):3582-3598. [\[CrossRef\]](#)
34. Chalasani N, Younossi Z, Lavine JE, et al. The diagnosis and management of non-alcoholic fatty liver disease: practice Guideline by the American Association for the Study of Liver Diseases, American College of Gastroenterology, and the American Gastroenterological Association. *Hepatology.* 2012;55(6):2005-2023. [\[CrossRef\]](#)
35. Bartlett JW, Frost C. Reliability, repeatability and reproducibility: analysis of measurement errors in continuous variables. *Ultrasound Obstet Gynecol.* 2008;31(4):466-475. [\[CrossRef\]](#)
36. Bland JM, Altman DG. JMAltmanDGMeasuring agreement in method comparison studies. *Stat Methods Med Res.* 1999;8(2):135-160. [\[CrossRef\]](#)
37. Bonferroni C. Il calcolo delle assicurazioni su gruppi di teste. *Tipogr Senat.* 1935:13-60.
38. Benjamini Y, Hochberg Y. Controlling the false discovery rate: a practical and powerful approach to multiple testing. *J R Stat Soc B.* 1995;57(1):289-300. [\[CrossRef\]](#)
39. Ferraioli G, Tinelli C, Dal Bello B, et al. Accuracy of real-time shear wave elastography for assessing liver fibrosis in chronic hepatitis C: a pilot study. *Hepatology.* 2012;56(6):2125-2133. [\[CrossRef\]](#)
40. Hudson JM, Milot L, Parry C, Williams R, Burns PN. Inter- and intra-operator reliability and repeatability of shear wave elastography in the liver: a study in healthy volunteers. *Ultrasound Med Biol.* 2013;39(6):950-955. [\[CrossRef\]](#)
41. Fang C, Konstantatou E, Romanos O, Yusuf GT, Quinlan DJ, Sidhu PS. Reproducibility of 2-dimensional shear wave elastography assessment of the liver: a direct comparison with point shear wave elastography in healthy volunteers. *J Ultrasound Med.* 2017;36(8):1563-1569. [\[CrossRef\]](#)
42. Mulabecirovic A, Mjelle AB, Gilja OH, Vesterhus M, Havre RF. Liver elasticity in healthy individuals by two novel shear-wave elastography systems—comparison by age, gender, BMI and number of measurements. *PLoS One.* 2018;13(9):e0203486. [\[CrossRef\]](#)
43. Gatos I, Drazinos P, Yarmenitis S, Theotokas I, Zoumpoulis PS. Comparison of sound touch elastography, shear wave elastography and vibration-controlled transient elastography in chronic liver disease assessment using liver biopsy as the “reference standard”. *Ultrasound Med Biol.* 2020;46(4):959-971. [\[CrossRef\]](#)
44. Jakovljevic M, Hsieh S, Ali R, Chau Loo Kung GC, Hyun D, Dahl JJ. Local speed of sound estimation in tissue using pulse-echo ultrasound: model-based approach. *J Acoust Soc Am.* 2018;144(1):254. [\[CrossRef\]](#)
45. Sehgal CM, Brown GM, Bahn RC, Greenleaf JF. Measurement and use of acoustic nonlinearity and sound speed to estimate composition of excised livers. *Ultrasound Med Biol.* 1986;12(11):865-874. [\[CrossRef\]](#)
46. Bamber JC, Hill CR. Acoustic properties of normal and cancerous human liver—I. Dependence on pathological condition. *Ultrasound Med Biol.* 1981;7(2):121-133. [\[CrossRef\]](#)
47. Gatos I, Tsantis S, Spiliopoulos S, et al. Temporal stability assessment in shear wave elasticity images validated by deep learning neural network for chronic liver disease fibrosis stage assessment. *Med Phys.* 2019;46(5):2298-2309. [\[CrossRef\]](#)
48. Gatos I, Tsantis S, Skouroliakou A, Theotokas I, Zoumpoulis PS, Kagadis GC. Optimal Elasticity cut-off value for discriminating Healthy to Pathological fibrotic patients employing Fuzzy C-Means automatic segmentation in Liver Shear Wave elastography images. *J Phys Conf Ser.* 2015;637:12008. [\[CrossRef\]](#)
49. Jung CH, Rhee EJ, Kwon H, Chang Y, Ryu S, Lee WY. Visceral-to-subcutaneous abdominal fat ratio is associated with nonalcoholic fatty liver disease and liver fibrosis. *Endocrinol Metab (Seoul).* 2020;35(1):165-176. [\[CrossRef\]](#)
50. Patijn J. Reproducibility and validity studies of diagnostic procedures in manual/musculoskeletal medicine. In: Hutson M, Ellis R, eds. *Textb. Musculoskelet.* 3rd ed, International Federation for Manual/Musculoskeletal Medicine Oxford University Press; 2006:550.